Direct in vivo monitoring of sarcoplasmic reticulum Ca^{2+} and cytosolic cAMP dynamics in mouse skeletal muscle

Rüdiger Rudolf,[1,2] Paulo J. Magalhães,[1] and Tullio Pozzan[1,2]

[1]Department of Biomedical Sciences, University of Padua, I-35121 Padua, Italy
[2]Venetian Institute of Molecular Medicine, I-35129 Padua, Italy

Skeletal muscle contraction depends on the release of Ca^{2+} from the sarcoplasmic reticulum (SR), but the dynamics of the SR free Ca^{2+} concentration ($[Ca^{2+}]_{SR}$), its modulation by physiological stimuli such as catecholamines, and the concomitant changes in cAMP handling have never been directly determined. We used two-photon microscopy imaging of GFP-based probes expressed in mouse skeletal muscles to monitor, for the first time in a live animal, the dynamics of $[Ca^{2+}]_{SR}$ and cAMP. Our data, which were obtained in highly physiological conditions, suggest that free $[Ca^{2+}]_{SR}$ decreases by ~50 μM during single twitches elicited through nerve stimulation. We also demonstrate that cAMP levels rise upon β-adrenergic stimulation, leading to an increased efficacy of the Ca^{2+} release/reuptake cycle during motor nerve stimulation.

Introduction

Excitation–contraction coupling in skeletal muscle depends on motor neuron–induced cell depolarization and the subsequent interaction between the dihydropyridine receptor (DHPR) and the ryanodine receptor (RYR), resulting in the release of Ca^{2+} from the terminal cisternae of the sarcoplasmic reticulum (SR). Although much has been done in this field, studies of the quantitative aspects and kinetics of the concentration of free Ca^{2+} in the SR lumen ($[Ca^{2+}]_{SR}$) have been marred by technical challenges. Most of the available data come from biochemical studies on isolated fractions (Volpe and Simon, 1991), x-ray microanalysis studies on rapidly frozen samples (Somlyo et al., 1981), or extrapolations measuring the rise of cytosolic $[Ca^{2+}]$ ($[Ca^{2+}]_c$; Baylor and Hollingworth, 2003). Recently, direct monitoring of $[Ca^{2+}]_{SR}$ made use of the fluorescent dyes fluo-5N (Kabbara and Allen, 2001) or mag-indo-1 (Launikonis et al., 2005) in isolated frog muscle fibers. These approaches still suffer from major drawbacks; the subcellular localization of the dyes is not SR specific, they are difficult to apply to live animals, and, thus far, no $[Ca^{2+}]_{SR}$ kinetics during excitation–contraction coupling with high temporal resolution have been determined. Cameleon Ca^{2+} sensors potentially overcome most of these problems. First, as they are genetically encoded, they can be selectively targeted to subcellular compartments. Second, their ratiometric nature ensures that changes in probe quantity and movement artifacts are inherently corrected (Rudolf et al., 2004). Third, they can be introduced into intact tissues and organisms by standard techniques (Rudolf et al., 2004). Finally, the recent molecular engineering of cameleons have functionally silenced the two central domains (i.e., CaM and the M13 peptide), rendering these probes virtually inert as cellular signaling molecules while maintaining their Ca^{2+}-sensing properties (Palmer et al., 2004).

Using an SR-targeted cameleon and two-photon confocal microscopy in live mouse, we have addressed two unsolved issues in muscle physiology: (1) direct quantitative measurement of the kinetics and amplitude of $[Ca^{2+}]_{SR}$ transients during single twitches and tetanic stimulation, and (2) the effect of β-adrenergic stimulation on SR Ca^{2+} handling. It is known that the force of contraction can be enhanced by β-receptor agonists in both heart and skeletal muscle (Cairns and Dulhunty, 1993b). In cardiac muscle, it involves PKA-dependent phosphorylation of troponin I (Zhang et al., 1995), DHPR (Bean et al., 1984), phospholamban (Lindemann et al., 1983), and RYR II (Yoshida et al., 1992). In skeletal muscle, the mechanism is less studied, but, as in the heart, it seems to rely on PKA-dependent phosphorylation of different targets, such as DHPR (Sculptoreanu et al., 1993) and RYR I (Sonnleitner et al., 1997). Regarding RYR I in particular, it is still a matter

Correspondence to Rüdiger Rudolf: ruediger.rudolf@itg.fzk.de

Abbreviations used in this paper: CPA, cyclopiazonic acid; DHPR, dihydropyridine receptor; K_d, apparent dissociation constant; PB, phosphate buffer; PKA, protein kinase A; RYR, ryanodine receptor; SERCA, sarcoendoplasmic reticulum Ca^{2+} ATPase; ROI, regions of interest; SR, sarcoplasmic reticulum; TA, tibialis anterior.

The online version of this article contains supplemental material.

The Journal of Cell Biology, Vol. 173, No. 2, April 24, 2006 187–193
http://www.jcb.org/cgi/doi/10.1083/jcb.200601160

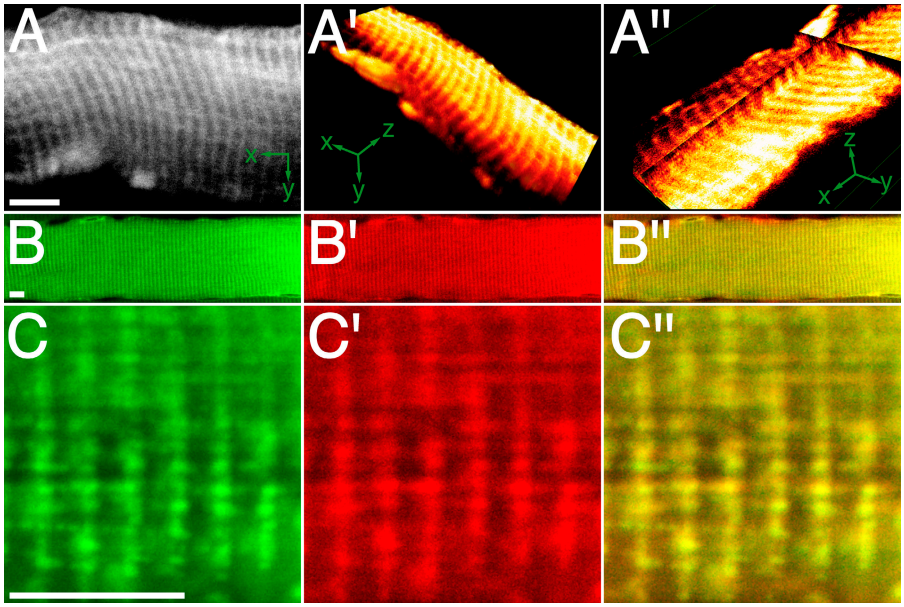

Figure 1. **D1ER is localized in the SR.** TA muscle was transfected with cDNA encoding D1ER. 2 wk later, optical sections were made in situ with two-photon microscopy (A–A″) or with confocal microscopy on longitudinal cryosections immunostained for SERCA 1 (B–C″). (A) Optical section of a single fiber (x-y orientation as indicated). (A′) 3D reconstruction of the fiber. (A″) Multiplanar reconstruction showing the optical plane in A as basal plate and the fluorescence signals in the z-dimension along the cross-shaped sheer plan (x-y-z orientation as indicated). A′ and A″ were made with OsiriX software. (B–C″) Fluorescence signals of D1ER (B and C, green), SERCA 1 immunostaining (B′ and C′, red), and overlay (B″ and C″, yellow). Bars, 10 μm.

of discussion whether phosphorylation of the channel is physiologically relevant (Sonnleitner et al., 1997; Blazev et al., 2001).

We demonstrate not only that a massive decrease of $[Ca^{2+}]_{SR}$ occurs during tetanic stimulation in vivo, but also that a substantial drop is elicited even during single muscle twitches. Using Epac1–cAMP sensor (Nikolaev et al., 2004), we show the first dynamic measurement of [cAMP] in a live animal and provide direct evidence that during β-adrenergic force potentiation the $[Ca^{2+}]_{SR}$ at rest, as well as the SR Ca^{2+} efflux and reuptake, are markedly increased.

Results and discussion

Expression of YC6.2ER and D1ER

Tibialis anterior (TA) muscles were transfected in vivo with cDNA encoding YC6.2ER or D1ER, which was targeted to the SR, as previously described (Rudolf et al., 2004). As shown in Fig. 1 (A–C″) for D1ER, the probe exhibited the typical striation pattern for SR. This pattern was always observed for D1ER, whereas YC6.2ER showed a more diffuse staining when strongly overexpressed. Data obtained with YC6.2ER was similar to that with D1ER; given the precise localization pattern of D1ER, however, only data with this probe is included in our study. Fig. 1 (B–C″) depicts confocal images of longitudinal slices of muscles transfected with D1ER (Fig. 1, B and C, green) and immunostained against sarcoendoplasmic reticulum Ca^{2+}-ATPase (SERCA) type 1 (Fig. 1, B′ and C′, red). The overlay shows the colocalization of the two proteins (Fig. 1, B″ and C″). This colocalization, along with the functional data revealing a drop in $[Ca^{2+}]_{SR}$ upon stimulation (see the following section), shows that D1ER is correctly targeted when expressed in live mouse skeletal muscle.

Strong $[Ca^{2+}]_{SR}$ decrease upon single twitch contraction

To quantify the drop of $[Ca^{2+}]_{SR}$ upon contraction, we studied the probe response at a stimulation frequency of 1 Hz. The background-subtracted YFP/CFP ratio images were scanned along the fiber length in 10-ms windows; in parallel, fiber deflection was measured as an indicator of muscle contraction (Fig. 2 A). The fibers exhibited a twitch profile of ∼100 ms in duration, which is typical of fast-twitch fibers and is as expected for this muscle. The ratio changes followed almost exactly the kinetics of fiber deflection, with the drop in ratio clearly preceding muscle contraction. However, the nadir in $[Ca^{2+}]_{SR}$, as measured with D1ER, is reached ∼30 ms after the start of contraction, which is similar to the time course of $[Ca^{2+}]_c$ rises that was previously measured (Rudolf et al., 2004), but definitively slower than the time-to-peak level in $[Ca^{2+}]_c$ as measured with a fast Ca^{2+} indicator (Baylor and Hollingworth, 2003). This discrepancy may be attributable to a variety of factors. First, a relatively slow dissociation of Ca^{2+} and conformational change of the cameleon may lead to a delay between the actual drop in $[Ca^{2+}]_{SR}$ and the decrease in fluorescence resonance energy transfer. We do not consider this possibility very likely because, according to fast kinetics measurements in vitro (Palmer et al., 2004), the dissociation rate constant (k_{off}) of D1ER is 256 s^{-1} and, thus, the indicator should be able to monitor a faster drop if it occurred; indeed, we calculated an even higher apparent dissociation constant (K_d) in HeLa cells than the one previously determined in vitro (Fig. S1, available at http://www.jcb.org/cgi/content/full/jcb.200601160/DC1), but the k_{off} could not be measured in situ. Second, the signal reflects the mean of the whole SR, as it is localized not only in the terminal cisternae but also, as suggested by the colocalization of the probe with SERCA 1 (Fig. 1, B″ and C″), in the longitudinal SR; in the latter, the changes in $[Ca^{2+}]_{SR}$ may be smaller and delayed. Third, the kinetics shown may reflect the actual situation, indicating that a decrease of $[Ca^{2+}]_{SR}$ may also continue during the decay phase of $[Ca^{2+}]_c$.

The maximal drops in absolute YFP/CFP ratio from the baseline differed considerably between different analyzed fibers, ranging from ∼3–25% of the initial value. The calibration

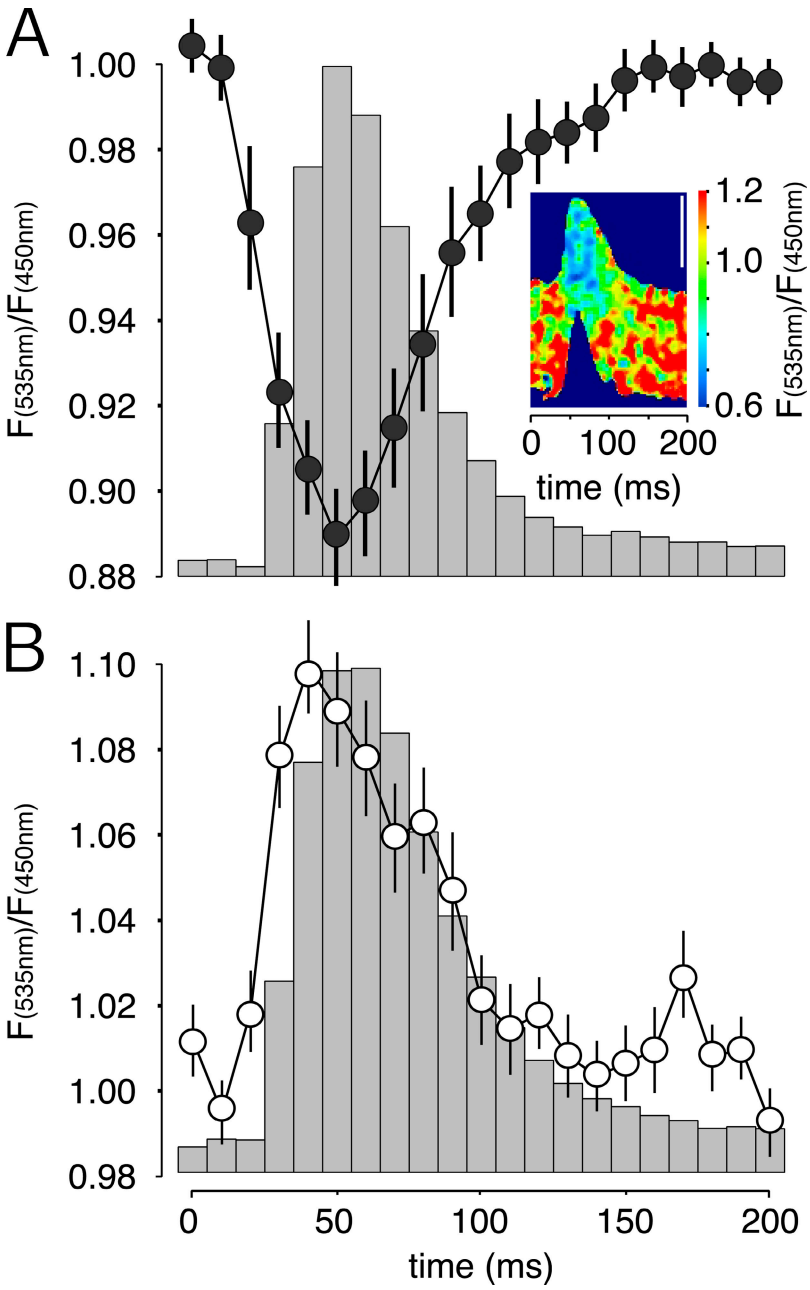

Figure 2. **D1ER reveals transient decreases of $[Ca^{2+}]_{SR}$ during single twitches in situ.** TA muscle was transfected with cDNA encoding D1ER (A) or YC2 (B). Fluorescence signals were monitored in situ during contraction, and the stimulation frequency was 1 Hz. Graphs show $[Ca^{2+}]_{SR}$ (A) or $[Ca^{2+}]_c$ (B) transients as measured by decrease or increase, respectively, of the YFP/CFP ratio normalized to the values in the relaxed state. Data are mean ± SEM. $n = 5$ fibers. 15 twitches per fiber were averaged. The contraction profile corresponding to the Ca^{2+} transients is indicated by the columns. The inset image in A shows a D1ER-expressing muscle fiber during contraction, with the YFP/CFP ratio indicated by pseudocolors (color scale, right). Bar, 50 μm.

of ratio signals into absolute $[Ca^{2+}]$ was derived from in situ measurements in culture cells (Fig. S1). Based on the known properties of D1ER and assuming a 200-μM K_d for Ca^{2+} within the SR lumen (which is higher than that calculated in vitro; Fig. S1), the basal $[Ca^{2+}]_{SR}$ was 308 ± 30 μM and exhibited a drop during single twitches of 53 ± 6 μM (for both, mean ± SEM; $n = 18$ fibers).

Effects of the partial inhibition of the SERCA

We then tested the effect of partial inhibition of the SERCA, using an appropriate dose of cyclopiazonic acid (CPA) to verify the importance of the SERCA on the kinetics of $[Ca^{2+}]_{SR}$ changes during stimulation. Intramuscular injection of CPA (100 μl of 100 μM CPA) caused a time-dependent drop of YFP/CFP ratio that typically stabilized ∼30–40 min after application of the drug at a value of 1.87 ± 0.17 (mean ± SEM; $n = 3$ fibers), corresponding to ∼134 μM. Under these conditions, SERCA inhibition was only partial; we could repetitively induce fiber contraction (Fig. 3 A), whereas, as shown in skinned rat fibers, a muscle fiber may contract only few times after complete block of the SERCA (Posterino and Lamb, 2003). Indeed, nerve stimulation of fibers treated with this CPA concentration revealed an amplification of contraction intensity (Fig. 3 A), albeit the resting $[Ca^{2+}]_{SR}$ was significantly lower than in controls and the maximal level of $[Ca^{2+}]_{SR}$ decrease was reduced (Fig. 3 B, top). In parallel experiments, we confirmed that the peak level in $[Ca^{2+}]_c$, as measured with cameleon YC2, is increased by this CPA treatment (unpublished data). Fiber contractions upon a single nerve impulse in the presence of CPA (Fig. 3 B)

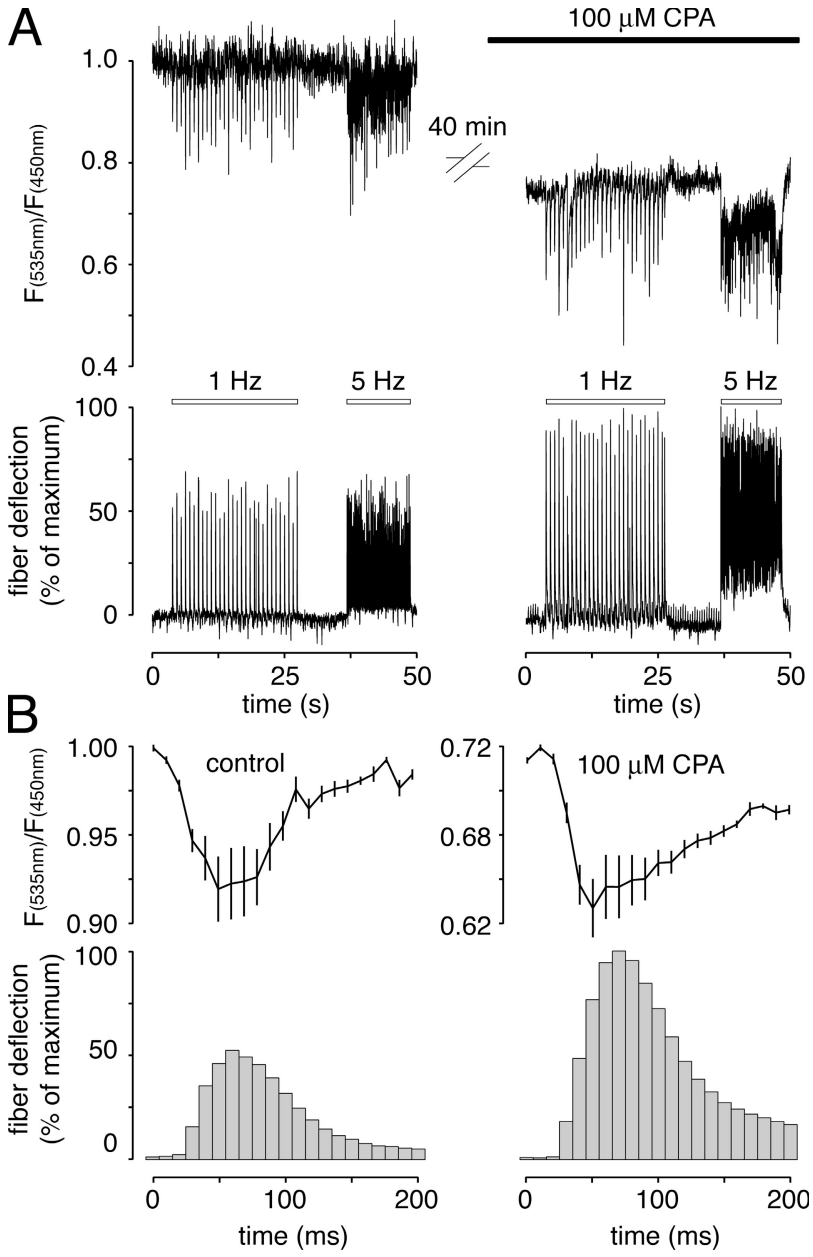

Figure 3. **Effects of partial inhibition of the SERCA.** Conditions were as in Fig. 1. (A) YFP/CFP ratio (top) and contraction profile (bottom) of a single experiment, with stimulation frequencies of 1 or 5 Hz and injection of CPA as indicated. Values are normalized to the start of the experiment. (B, top) $[Ca^{2+}]_{SR}$ transients for control fibers and fibers treated with 100 μM CPA, as indicated. (bottom) The corresponding contraction profiles. Stimulation frequency was 1 Hz. For each experiment and condition, 25 individual twitches were averaged. Data shown represent mean ± SEM. $n = 4$ fibers. Values are normalized to control.

were also stronger than in control conditions; similar results have been obtained in another study (Rios and Stern, 1997). This cannot be easily explained if all Ca^{2+} release from the SR was caused by electromechanical coupling, i.e., if it occurred only during the action potential. In this case, one would expect the contraction and rise in $[Ca^{2+}]_c$ to be the same, or smaller, in CPA-treated muscle compared with controls. Several possibilities, which are not mutually exclusive, may be suggested: (1) a reduced cytoplasmic Ca^{2+} buffering in the presence of CPA, caused by a slight increase in $[Ca^{2+}]_c$ (with partial saturation of $[Ca^{2+}]_c$ buffers); a small capacitative Ca^{2+} entry might be activated under these experimental conditions (Kurebayashi and Ogawa, 2001); however, we found no significant increase in basal $[Ca^{2+}]_c$ in the presence of CPA (unpublished data); (2) a reduced contribution of the Ca^{2+}-binding activity of the SERCA, given that SERCA bound to CPA are in a low Ca^{2+} affinity conformation (Goeger and Riley, 1989); and (3) that the massive release caused by electromechanical coupling was followed by a small, but prolonged, release of Ca^{2+} (apparently, as monitored with D1ER), which is possibly a consequence of Ca^{2+}-induced Ca^{2+} release. A slow release could be partially counteracted by the SERCA activity and, thus, be unmasked in fibers treated with CPA. The role and existence of Ca^{2+}-induced Ca^{2+} release in fast skeletal muscle is surely of minor relevance (Shirokova et al., 1996, 1998; Rios and Stern, 1997), but to our knowledge it has never been completely excluded.

Ca^{2+} release from the SR upon β-adrenergic potentiation in situ

Our experimental setup enabled us to address an unanswered question of the utmost biological relevance: the role of the SR in β-adrenergic force potentiation. First, we directly studied the

effect of isoproterenol, which is a β−adrenergic agonist, on [cAMP] by transfecting TA muscles with Epac1–cAMP sensor (Nikolaev et al., 2004). The subcellular distribution of fluorescence was homogeneous (cytoplasmic) within the fibers (Fig. 4 A). We found a highly reproducible rise in [cAMP] upon injection of isoproterenol, as shown by the increase of the CFP/YFP ratio to 1.33 ± 0.03 (mean ± SEM; $n = 8$ fibers; data normalized to control; Fig. 4 B). The rise was already maximal 10 min after application of the drug and decreased slightly thereafter (Fig. 4 B). Similar results were obtained with another fluorescent PKA-based cAMP probe (Zaccolo and Pozzan, 2002) and upon injection of high doses of forskolin (250 μM); given the probe's ∼2-μM cAMP K_d (Nikolaev et al., 2004), the rise in [cAMP] that is attributable to β-adrenergic stimulation is likely in the micromolar range.

As shown in Fig. 4 C (bottom), the application of isoproterenol also led to a larger fiber deflection, which is indicative of the expected force potentiation. This increase in single-twitch amplitude was paralleled by four interesting phenomena. First, the basal-normalized YFP/CFP ratio increased from 1.00 ± 0.02% to 1.06 ± 0.01% (mean ± SEM; $n = 3$ fibers) after injection of isoproterenol (Fig. 4 C, top). According to the calibration procedure described in the supplemental material, this would account for a rise in $[Ca^{2+}]_{SR}$ from ∼278 to ∼311 μM. Second, the decrease of YFP/CFP ratio during single twitches was enhanced in the presence of isoproterenol without interim stimulation (Fig. 4 C, top), accounting for drops in $[Ca^{2+}]_{SR}$ of ∼65 and ∼99 μM in the absence and presence of isoproterenol, respectively; this effect was even stronger upon 50 Hz stimulation, where the corresponding changes were calculated to be ∼83 and ∼153 μM. Third, the kinetics of the Ca^{2+}-release/reuptake cycle during single twitches in the presence of isoproterenol had the same duration as in controls (160 ms). Thus, the rise in [cAMP], presumably via PKA-dependent phosphorylation, increases Ca^{2+} release from the SR, but does not change the kinetics of release/reuptake. Finally, although the drop in $[Ca^{2+}]_{SR}$ was higher in the presence of isoproterenol, the time constants from peak to half-maximal recovery were virtually identical in the absence (35 ms) and presence (36 ms) of the adrenergic stimulus. Thus, during the same time period more Ca^{2+} is taken up by the SR in fibers stimulated by isoproterenol compared with controls.

In summary, the data presented show that stimulation of β-adrenergic receptors in skeletal muscles leads to a major and prolonged rise of [cAMP] accompanied by an increase of basal $[Ca^{2+}]_{SR}$ and a drop in $[Ca^{2+}]_{SR}$ during contraction. The increased fiber contraction is clearly dependent on the larger Ca^{2+} release because previous work has shown that, unlike in cardiac fibers, cAMP-dependent PKA activation does not modify the Ca^{2+} sensitivity of the contractile apparatus (Fabiato and Fabiato, 1978; Cairns and Dulhunty, 1993a). In particular, only myosin-binding protein C and troponin I of cardiac muscle may be phosphorylated by PKA (Tong et al., 2004).

Regarding the effect of isoproterenol on Ca^{2+} release, different, nonmutually exclusive explanations may be considered. First, a higher basal $[Ca^{2+}]_{SR}$ might account for a larger release of Ca^{2+} during contraction. However, no correlation between

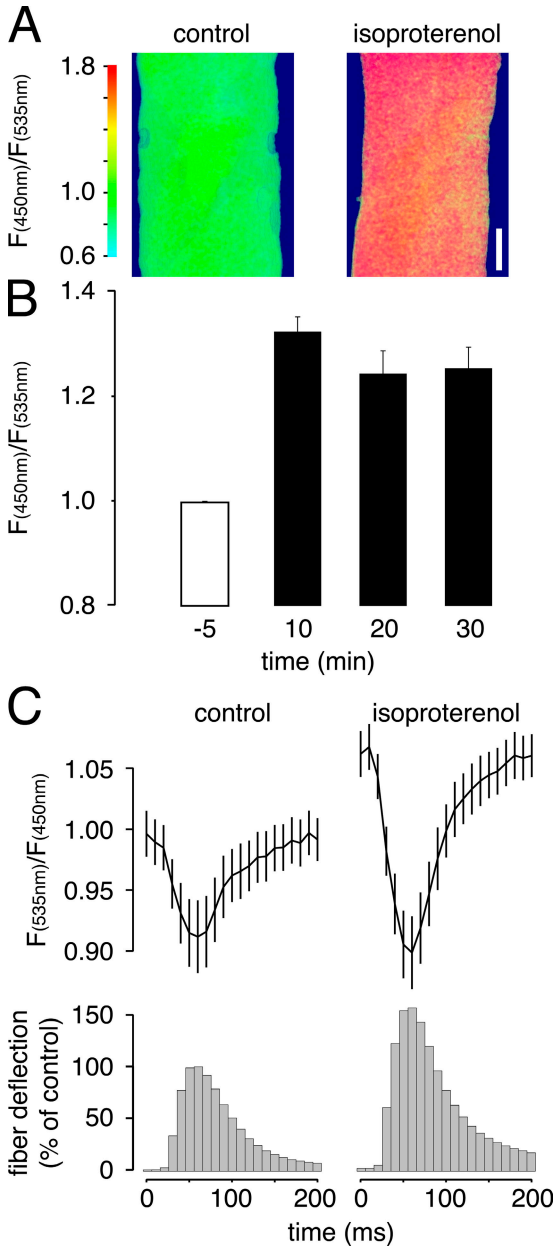

Figure 4. **In situ β-adrenergic potentiation involves rise of [cAMP] and amplification of Ca^{2+} release and reuptake from the SR.** TA muscle was transfected with cDNA coding for Epac1–cAMP sensor (A and B) or D1ER (C), fluorescence signals were monitored in situ. (A) Epac1–cAMP sensor–expressing fiber before (left) and 10 min after (right) injection of isoproterenol; the CFP/YFP ratio is indicated by pseudocolors (color scale, left). Bar, 10 μm. (B) Epac1–cAMP sensor response to isoproterenol. Data shown represent mean ± SEM. $n = 8$ fibers. Values are normalized to control and the time from injection is as indicated. (C) Stimulation frequency was 1 Hz. (top) $[Ca^{2+}]_{SR}$ transients of the same fibers before (control) and after (isoproterenol) treatment with isoproterenol. (bottom) Corresponding contraction profiles. For each experiment and condition, 25 individual twitches were averaged. Data shown represent mean ± SEM. $n = 3$ fibers. Values are normalized to control.

basal $[Ca^{2+}]_{SR}$ and the drop during contraction was observed; neither by ourselves (Fig. S2, B and C, available at http://www.jcb.org/cgi/content/full/jcb.200601160/DC1) nor in a previous study (Posterino and Lamb, 2003). Second, the increased Ca^{2+} efflux could be attributable to direct cAMP/PKA-dependent

activation of RYR I; this possibility has been previously proposed (Sonnleitner et al., 1997; Blazev et al., 2001), but no convincing evidence has been provided. Third, and most likely, it could be caused by PKA-dependent phosphorylation of DHPR that increases its coupling to RYR I. Strong evidence supporting this mechanism has been obtained in myoblasts (Sculptoreanu et al., 1993).

The effect of β-adrenergic stimulation on Ca^{2+} accumulation was unexpected for fast skeletal muscle, which is known to be devoid of phospholamban (Vangheluwe et al., 2005). Evidence supporting a role for cAMP in SERCA stimulation has been described in the skinned fibers of cat (Fabiato and Fabiato, 1978), but this finding has been neglected for almost 30 yr. A simple, conservative explanation may be an indirect effect of cAMP/PKA on SERCA activity, mediated by PKA activation of glycogen metabolism (Gross et al., 1976); both pyruvate (Hermann et al., 2000) and local ATP generation by SR-bound glycolytic enzymes appear particularly important for the activity of SERCA (Korge and Campbell, 1994). Increased availability of glucose (and, thus, ATP) may explain the higher Ca^{2+} loading of the SR upon β-adrenergic stimulation.

Materials and methods

Expression plasmids, antibodies, and chemicals
Transfection experiments used the following constructs in pcDNA3 (Invitrogen): YC2, D1ER, and Epac1–cAMP sensor were gifts from R.Y. Tsien (University of California, San Diego, San Diego, CA) and M.J. Lohse (University of Würzburg, Würzburg, Germany). The A23187, ascorbic acid, CPA, digitonin, histamine, isoproterenol, and thapsigargin (all from Sigma-Aldrich) used were of the highest available grade. All injected drugs and cDNAs were diluted in sterile physiological solution (0.9% NaCl). SERCA 1 antibody (clone VE121G9) was purchased from Affinity BioReagents and Alexa Fluor 568 goat anti–mouse IgG was purchased from Invitrogen.

Animals
All experiments used C57BL/10 mice (aged 6–12 mo; Charles River Italia). Animal handling was approved by the local authority for veterinary services, in accordance with Italian law. For anesthesia, Rompun (Bayer) and Zoletil 100 (Laboratoires Virbac) were injected i.p.

Transfection
Transfection was carried out using an electroporation-based method of the TA muscle, as previously described (Rudolf et al., 2004).

Slice preparation and immunohistochemistry
For immunostaining, muscles were first stretched, fixed overnight at 4°C in 4% paraformaldehyde in 0.1 M phosphate buffer (PB), and dehydrated in 10% sucrose/PB; they were then snap frozen in liquid nitrogen–cooled isopentane. The muscle was embedded in Jung tissue-freezing medium and 10-μm-thick cryosections were prepared using a cryostat (model CM1850; Leica). After drying, the sections were quenched with 50 mM NH_4Cl/PB and permeabilized with 0.1% Triton X-100/PB. Sections were then rinsed with PB, blocked with 0.2% gelatin/PB and incubated with anti-SERCA 1 antibody (1:500, diluted in 0.2% gelatin/PB) overnight at 4°C. Sections were blocked again with 0.2% gelatin/PB and incubated with the secondary antibody (1:250, diluted in 0.2% gelatin/PB) for 2 h. Finally, the preparations were rinsed in 0.2% gelatin/PB and PB and mounted in Mowiol.

Confocal analysis of immunostainings
Confocal images of immunostained sections were obtained with a microscope (Radiance 2100MP; BioRad Laboratories) equipped with an Ar (488-nm line) laser and a HeNe laser (543-nm line), a 60×/1.4 NA objective (Nikon), a 560DCLPXR dichroic mirror, HQ515/30 and E570LP emission filters (Chroma Technology Corp.) for the detection of cameleon, and Alexa Fluor 568 fluorescence signals. Images were taken at 1,024 × 1,024 pixel resolution and 50 lines s^{-1} scan speed.

In vivo two-photon microscopy
This procedure was performed as previously described (Rudolf et al., 2004), with minor modifications. Unless otherwise indicated, video microscopy was performed at 256 × 256 pixels with a 1.95-Hz acquisition frequency. For $[Ca^{2+}]_{SR}$ studies, images were acquired at 1,024 × 1,024 pixels at 166 lines s^{-1}. Drug injection (1 mM CPA, 100 μM CPA, or 10 μM isoproterenol + 1 mM ascorbic acid) was performed locally using a 30-gauge needle (Artsana) with a typical volume of 100 μl. To allow the muscle to recover from the injection-induced swelling, microscopic observation was interrupted for at least 5 min.

Data analysis of ratiometric images
Datasets were analyzed essentially as previously described (Rudolf et al., 2004), using ImageJ software (National Institutes of Health). Fibers were oriented in the microscopic field with the longitudinal axis perpendicular to the line scan direction, matching the timeline to the long fiber axis. A mask containing the whole observed part of the fiber was created from the corresponding median-filtered YFP video by intensity thresholding. Next, both CFP and YFP videos were mean filtered (1 pixel kernel) to suppress hot pixel noise, background intensity was subtracted when necessary, and the mask was applied. For the data shown in Fig. S1, the mean CFP and YFP values were determined inside the mask region; subsequent calculations and graphs used Excel 2002 (Microsoft). Ratio plots were normalized using the last 10 images preceding the first contraction as reference values. The ratio values during single twitches, such as in Figs. 2–4, were obtained as follows. A YFP/CFP ratio video was created by applying the custom-made ImageJ plug-in Ratio Plus. Ratio values were then determined along the fiber length in regions of interest (ROIs) with a width of 5 pixels, equaling 10-ms time frames. The background value at any ROI was calculated as the mean at that position in the 10 frames preceding the first contraction and was subtracted from the ROIs obtained during contraction using the formula: $n_{i+a} = (x_{i+a} + m - m_a)/m_c$, where n_{i+a} is the normalized ratio value at point i + a, x_{i+a} is the measured ratio value at point i + a, m is the mean ratio value along the whole fiber length, and m_a is the mean ratio value at point a. In Fig. 2, m_c is equal to m, whereas in Figs. 3 and 4 it is equal to m of the corresponding controls. In parallel, the relative fiber deflection was determined using the last frame before the first contraction as a blank. For the average calculations shown in Figs. 2–4, individual twitches were synchronized by setting the first ROI with deflection as the start of contraction. For the timelines shown in Fig. 3 A, subsequent frames were treated as continuous in time; this assumption is valid because the time-lapse between the last scan line of an image and the first one of the following frame was of the same order as the jump from one line to the next in the same frame, and because contractions that initiated in one frame and continued in a following frame, appeared smooth in procedure after recomposition, as executed in Fig. 3 A.

Online supplemental material
Experiments showing the functionality and correction for movement artifacts of D1ER as well as a detailed description of D1ER in situ calibration are available online. Online supplemental material is available at http://www.jcb.org/cgi/content/full/jcb.200601160/DC1.

We thank Drs. M. Ikura, M.J. Lohse, RY. Tsien, and M. Brini for their generous gifts of plasmids and antibodies, and Drs. M. Mongillo, M. Zaccolo, D. Sandonà, E. Damiani, and A. Margreth for fruitful discussions.

R. Rudolf was supported by grants from the University of Padua and the Deutsche Forschungsgemeinschaft (RU 923/1-1). The following grants to T. Pozzan also partially supported this work: Italian Telethon (grant 1226), Italian Association for Cancer Research, Italian Ministry of Universities (Special Projects Prin RBNE01ERXR-001 and 20033054449-001, and FIRB 2002053318-005), Italian Ministry of Health, and the CARIPARO foundation.

Submitted: 27 January 2006
Accepted: 16 March 2006

References

Baylor, S.M., and S. Hollingworth. 2003. Sarcoplasmic reticulum calcium release compared in slow-twitch and fast-twitch fibres of mouse muscle. *J. Physiol.* 551:125–138.

Bean, B.P., M.C. Nowycky, and R.W. Tsien. 1984. Beta-adrenergic modulation of calcium channels in frog ventricular heart cells. *Nature*. 307:371–375.

Blazev, R., M. Hussain, A.J. Bakker, S.I. Head, and G.D. Lamb. 2001. Effects of the PKA inhibitor H-89 on excitation-contraction coupling in skinned and intact skeletal muscle fibres. *J. Muscle Res. Cell Motil.* 22:277–286.

Cairns, S.P., and A.F. Dulhunty. 1993a. Beta-adrenergic potentiation of E-C coupling increases force in rat skeletal muscle. *Muscle Nerve*. 16:1317–1325.

Cairns, S.P., and A.F. Dulhunty. 1993b. The effects of beta-adrenoceptor activation on contraction in isolated fast- and slow-twitch skeletal muscle fibres of the rat. *Br. J. Pharmacol.* 110:1133–1141.

Fabiato, A., and F. Fabiato. 1978. Cyclic AMP-induced enhancement of calcium accumulation by the sarcoplasmic reticulum with no modification of the sensitivity of the myofilaments to calcium in skinned fibres from a yeast skeletal muscle. *Biochim. Biophys. Acta*. 539:253–260.

Goeger, D.E., and R.T. Riley. 1989. Interaction of cyclopiazonic acid with rat skeletal muscle sarcoplasmic reticulum vesicles. Effect on Ca2+ binding and Ca2+ permeability. *Biochem. Pharmacol.* 38:3995–4003.

Gross, S.R., S.E. Mayer, and M.A. Longshore. 1976. Stimulation of glycogenolysis by beta adrenergic agonists in skeletal muscle of mice with the phosphorylase kinase deficiency mutation (I strain). *J. Pharmacol. Exp. Ther.* 198:526–538.

Hermann, H.P., O. Zeitz, B. Keweloh, G. Hasenfuss, and P.M. Janssen. 2000. Pyruvate potentiates inotropic effects of isoproterenol and Ca(2+) in rabbit cardiac muscle preparations. *Am. J. Physiol. Heart Circ. Physiol.* 279:H702–H708.

Kabbara, A.A., and D.G. Allen. 2001. The use of the indicator fluo-5N to measure sarcoplasmic reticulum calcium in single muscle fibres of the cane toad. *J. Physiol.* 534:87–97.

Korge, P., and K.B. Campbell. 1994. Local ATP regeneration is important for sarcoplasmic reticulum Ca2+ pump function. *Am. J. Physiol.* 267:C357–C366.

Kurebayashi, N., and Y. Ogawa. 2001. Depletion of Ca2+ in the sarcoplasmic reticulum stimulates Ca2+ entry into mouse skeletal muscle fibres. *J. Physiol.* 533:185–199.

Launikonis, B.S., J. Zhou, L. Royer, T.R. Shannon, G. Brum, and E. Rios. 2005. Confocal imaging of [Ca2+] in cellular organelles by SEER, Shifted Excitation and Emission Ratioing of fluorescence. *J. Physiol.* 567:523–543.

Lindemann, J.P., L.R. Jones, D.R. Hathaway, B.G. Henry, and A.M. Watanabe. 1983. beta-Adrenergic stimulation of phospholamban phosphorylation and Ca2+-ATPase activity in guinea pig ventricles. *J. Biol. Chem.* 258:464–471.

Nikolaev, V.O., M. Bunemann, L. Hein, A. Hannawacker, and M.J. Lohse. 2004. Novel single chain cAMP sensors for receptor-induced signal propagation. *J. Biol. Chem.* 279:37215–37218.

Palmer, A.E., C. Jin, J.C. Reed, and R.Y. Tsien. 2004. Bcl-2-mediated alterations in endoplasmic reticulum Ca2+ analyzed with an improved genetically encoded fluorescent sensor. *Proc. Natl. Acad. Sci. USA*. 101:17404–17409.

Posterino, G.S., and G.D. Lamb. 2003. Effect of sarcoplasmic reticulum Ca2+ content on action potential-induced Ca2+ release in rat skeletal muscle fibres. *J. Physiol.* 551:219–237.

Rios, E., and M.D. Stern. 1997. Calcium in close quarters: microdomain feedback in excitation-contraction coupling and other cell biological phenomena. *Annu. Rev. Biophys. Biomol. Struct.* 26:47–82.

Rudolf, R., M. Mongillo, P.J. Magalhaes, and T. Pozzan. 2004. In vivo monitoring of Ca^{2+} uptake into mitochondria of mouse skeletal muscle during contraction. *J. Cell Biol.* 166:527–536.

Sculptoreanu, A., T. Scheuer, and W.A. Catterall. 1993. Voltage-dependent potentiation of L-type Ca2+ channels due to phosphorylation by cAMP-dependent protein kinase. *Nature*. 364:240–243.

Shirokova, N., J. Garcia, G. Pizarro, and E. Rios. 1996. Ca^{2+} release from the sarcoplasmic reticulum compared in amphibian and mammalian skeletal muscle. *J. Gen. Physiol.* 107:1–18.

Shirokova, N., J. Garcia, and E. Rios. 1998. Local calcium release in mammalian skeletal muscle. *J. Physiol.* 512:377–384.

Somlyo, A.V., H.G. Gonzalez-Serratos, H. Shuman, G. McClellan, and A.P. Somlyo. 1981. Calcium release and ionic changes in the sarcoplasmic reticulum of tetanized muscle: an electron-probe study. *J. Cell Biol.* 90:577–594.

Sonnleitner, A., S. Fleischer, and H. Schindler. 1997. Gating of the skeletal calcium release channel by ATP is inhibited by protein phosphatase 1 but not by Mg2+. *Cell Calcium*. 21:283–290.

Tong, C.W., R.D. Gaffin, D.C. Zawieja, and M. Muthuchamy. 2004. Roles of phosphorylation of myosin binding protein-C and troponin I in mouse cardiac muscle twitch dynamics. *J. Physiol.* 558:927–941.

Vangheluwe, P., M. Schuermans, E. Zador, E. Waelkens, L. Raeymaekers, and F. Wuytack. 2005. Sarcolipin and phospholamban mRNA and protein expression in cardiac and skeletal muscle of different species. *Biochem. J.* 389:151–159.

Volpe, P., and B.J. Simon. 1991. The bulk of Ca2+ released to the myoplasm is free in the sarcoplasmic reticulum and does not unbind from calsequestrin. *FEBS Lett.* 278:274–278.

Yoshida, A., M. Takahashi, T. Imagawa, M. Shigekawa, H. Takisawa, and T. Nakamura. 1992. Phosphorylation of ryanodine receptors in rat myocytes during beta-adrenergic stimulation. *J. Biochem. (Tokyo)*. 111:186–190.

Zaccolo, M., and T. Pozzan. 2002. Discrete microdomains with high concentration of cAMP in stimulated rat neonatal cardiac myocytes. *Science*. 295:1711–1715.

Zhang, R., J. Zhao, A. Mandveno, and J.D. Potter. 1995. Cardiac troponin I phosphorylation increases the rate of cardiac muscle relaxation. *Circ. Res.* 76:1028–1035.